Optical high-order harmonic generation as a structural characterization tool

Lei Jia [ORCID], Zhiya Zhang, D. Z. Yang, Yanqing Liu, and M. S. Si [ORCID][*]

Key Laboratory for Magnetism and Magnetic Materials of the Ministry of Education, Lanzhou University, Lanzhou 730000, China

G. P. Zhang[†]

Department of Physics, Indiana State University, Terre Haute, Indiana 47809, USA

Y. S. Liu [ORCID]

College of Physics and Electronic Engineering, Changshu Institute of Technology, Changshu 215500, China

Structural characterization is essential to material engineering, but few tools can detect structural properties in the time domain. High harmonic generation (HHG) emerges as a new frontier that touches the heart of condensed-matter physics from the symmetry to quantum geometrical nature of electrons, but its capability in structural characterization has not been materialized. Here, we establish a crucial connection between the symmetry of a material and the helicity of light. We employ monolayer MoS_2 as an example. We show that a linearly polarized laser pulse used in experiments is not ideal for structural characterization because it only generates in-plane anisotropy. It is the circularly polarized laser field that is capable of producing four distinctive HHG signals from the four phases of MoS_2. This finally links the laser helicity to the crystal structure. The results are generic and are not affected by the Berry curvature, the interband or intraband contribution. Our study unleashes the power of HHG as a structural characterization tool for technologically important materials.

I. INTRODUCTION

High harmonic generation (HHG) has emerged as a promising tool to study strong field effects and ultrafast electron dynamics in two-dimensional (2D) materials [1–3]. This inspires extensive investigations in 2D materials at attosecond timescales [3–8]. Recently, harmonic signals have been observed in graphene [9–11], MoS_2 [3,12–15], and CrI_3 [16], where the harmonic signals crucially depend on the crystal symmetry. In graphene, only odd harmonics appear owing to the inversion symmetry [10,11]. In contrast to graphene, even harmonics due to the broken inversion symmetry are observed in MoS_2 and CrI_3. The emerging even harmonics have attracted intense attention [3,12,13]. Liu and coauthors believed that the Berry curvature from the broken inversion symmetry gives rise to the even harmonics in MoS_2 [3]. However, their method ignores the effect of the interband polarization. Therefore, the correlation between the even harmonics and the Berry curvature in MoS_2 is still a matter of debate. It is also worth noting that some of symmetry properties of HHG summarized in the Supplementary Information of Ref. [3] seem to be inconsistent with those in the main text. To this end, focus has been on the $1H$-semiconducting phase [3,11–15,17], but MoS_2 has three other common crystalline phases of $1T$, $1T'$, and $1T_d$ [18]. The different phases have different electronic properties. For example, the $1T'$ phase has a large quantum spin Hall effect while the $1T$ phase is metallic

[19,20]. The existence of these rich phases broadens the scope of monolayer MoS_2. However, since the $1T'$ and $1T$ phases have similar crystal structures [20], how to distinguish them experimentally is extremely challenging. A similar phase transition is also found in $MoTe_2$ [7].

In this work, we demonstrate an unexplored capability of HHG to distinguish crystalline phases of MoS_2 through laser helicity. The crystal symmetry has a remarkable impact on HHG signals. We find that, when the laser is linearly polarized, even harmonics appear in $1H$ and $1T_d$ MoS_2 but disappear in $1T$ and $1T'$ MoS_2. But the huge difference in HHG between two laser polarizations, parallel and perpendicular to the in-plane mirror symmetry, cannot separate the $1T$ phase from the $1T'$ phase. This shows the limitation of linearly polarized light [3]. We find that only circularly polarized light can do the job, where the four phases exhibit four remarkably different harmonics. $1H$ MoS_2 only has $3n \pm 1$ harmonics in-plane (n is an integer), $1T$ MoS_2 only has the $6n \pm 1$ in-plane harmonics and $6n + 3$ out-of-plane harmonics, $1T'$ MoS_2 only has odd harmonics, and the $1T_d$ phase has both even and odd harmonics. These results show that the group symmetry difference leaves a distinctive hallmark on the harmonic signals that manifest themselves through laser helicity. This finding is expected to motivate further experimental investigations to develop HHG into a structure characterization tool at the ultrafast timescale.

II. THEORETICAL METHOD

To fully appreciate the power of HHG, we choose MoS_2 which has four crystalline phases and has a

[*]sims@lzu.edu.cn
[†]guo-ping.zhang@outlook.com

quasi-two-dimensional structure. We employ a generic Hamiltonian which reads

$$\mathscr{H} = \mathscr{H}_0 + \mathscr{H}_I(t), \qquad (1)$$

where $\mathscr{H}_0$ is the ground-state Hamiltonian that accounts for the electronic energy of the solid and $\mathscr{H}_I(t)$ is the interaction Hamiltonian between the system and the femtosecond laser pulse. Before calculating the HHG, we self-consistently solve the Kohn-Sham equation [21], which is implemented in WIEN2K [22]. Here, we ignore the crystal vibration induced by the irradiation of laser pulse. Once the calculation converges, we construct the density matrix of the ground state from $\rho_0 = |\Psi_{nk}\rangle\langle\Psi_{nk}|$, where Ψ_{nk} is the Bloch wave function of band n at crystal momentum k. We then obtain the dynamic density matrix by numerically solving the time-dependent Liouville equation $i\hbar\langle n\mathbf{k}|\partial\rho/\partial t|m\mathbf{k}\rangle = \langle n\mathbf{k}[\mathscr{H}, \rho]m\mathbf{k}\rangle$ [23]. Finally, HHG is computed by Fourier transforming the induced macroscopic polarization $\mathbf{P}(t) = \sum_k \mathrm{Tr}[\rho_k(t)\hat{\mathbf{P}}_k]$, with $\hat{\mathbf{P}}_k$ being the momentum operator. $\mathscr{H}_I(t)$ is generally spatiotemporal and thus includes all the dynamical properties as well as symmetries. Whenever $\mathscr{H}_I(t)$ is invariant under a symmetry operation, the HHG must follow strict selection rules.

III. PROOF OF PRINCIPLE AND COMPARISON WITH EXPERIMENT UNDER LINEARLY POLARIZED LIGHT

Monolayer MoS_2 has four phases: $1H$, $1T$, $1T'$, and $1T_d$. The most studied type is the $1H$ phase, but there has been no study of HHG on the other three types. The $1H$ phase has a point-group symmetry D_{3h} with an in-plane mirror symmetry [highlighted by the horizontal green line in Fig. 1(a)]. We show below crystal symmetries that manifest themselves in HHG through the selection rules. When the laser field is linearly polarized along the x axis (i.e., parallel to the mirror plane), only harmonics whose polarization is parallel to the field are generated from $1H$ MoS_2, where both even and odd harmonics are present [see Fig. 1(a)]. By contrast there is no signal perpendicular to the laser field. Since the wave propagation direction must be perpendicular to the electric-field vector, harmonic signals can be spatially separated and detected by different cameras, as demonstrated in Fig. 1(a). This greatly eases the experimental detection.

However, when the laser field is polarized along the y axis (perpendicular to the mirror plane), the situation is entirely different. $1H$ MoS_2 emits harmonics in both the parallel and perpendicular directions [see Fig. 1(b)], with the parallel component being odd while the perpendicular one is even, fully consistent with the experimental results reported by Liu and coauthors [3]. But Table 1 in the Supplementary Information [3] contains an error in this configuration, where both even and odd harmonics are listed. The other three phases of MoS_2 yield slightly different HHG with an in-plane anisotropy under linearly polarized laser (see the Supplemental Material [22]).

IV. HIGH HARMONIC GENERATION UNDER CIRCULARLY POLARIZED (σ) LIGHT

There has been no experimental investigation of HHG in MoS_2 under σ light, despite the recognized importance
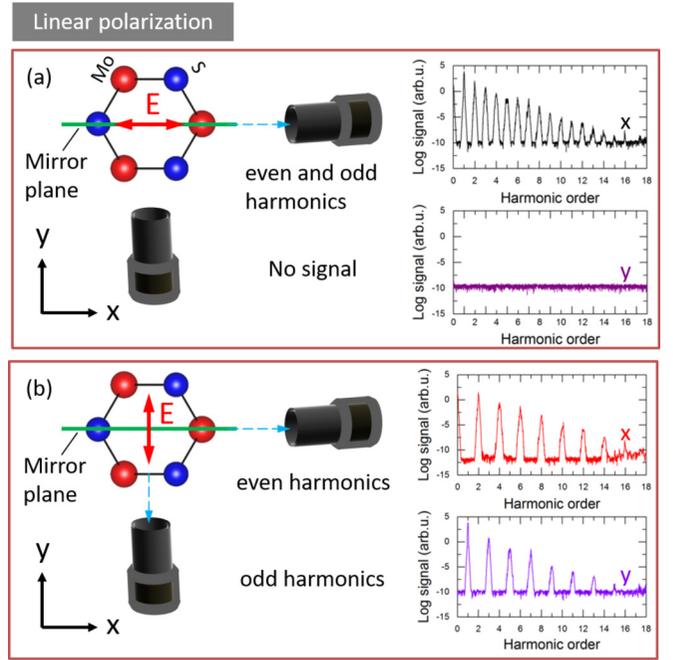
FIG. 1. High harmonic signals from $1H$ MoS_2 under two configurations: (a) parallel and (b) perpendicular. For the parallel configuration, the parallel polarization component has both even and odd harmonic signals. By contrast, for the perpendicular configuration, the cross-harmonic signals are induced, where the even harmonics appear for the parallel component while the odd harmonics appear for the perpendicular component. The cameras are placed at the same plane of the monolayer MoS_2. The dashed lines represent the emitted signals of HHG. The parameters of the laser field are taken as $A_0 = 0.03$ V fs/Å, $\hbar\omega = 1.0$ eV, and $\tau = 60$ fs.

of light helicity [3,24]. In our study, when we use σ light within the xy plane and, to our amazement, we find that four types of MoS_2 produce four distinctive harmonic signals. For instance, $1H$ MoS_2 presents signals with polarization parallel and perpendicular to the laser field, but has no out-of-plane signal along the z axis [see Fig. 2(a)]. We also find that the harmonic orders are peculiar: only $(3n - 1)$- and $(3n + 1)$-order harmonics appear, while $3n$-order harmonics are missing, where n is an integer. However, this is no longer the case for $1T$ MoS_2. The harmonic orders of the in-plane polarization components are $6n + 1$ and $6n - 1$. The out-of-plane polarization component is of order $6n + 3$. For $1T'$ MoS_2, in contrast to the two cases above, the harmonic order in an arbitrary direction is odd [Fig. 2(c)]. For $1T_d$ MoS_2, each polarization component contains both even and odd harmonics [Fig. 2(d)]. Such different HHG from the four phases of MoS_2 demonstrate that HHG from the circularly polarized light is capable of distinguishing different crystalline phases of monolayer MoS_2. Our finding now connects a pure theoretical result [6] with the structural characterization. In other words, the experimental pattern of HHG combined with the symmetries behind the selective rules would identify the phase of a material. This serves as the basis of HHG as a structure characterization tool.
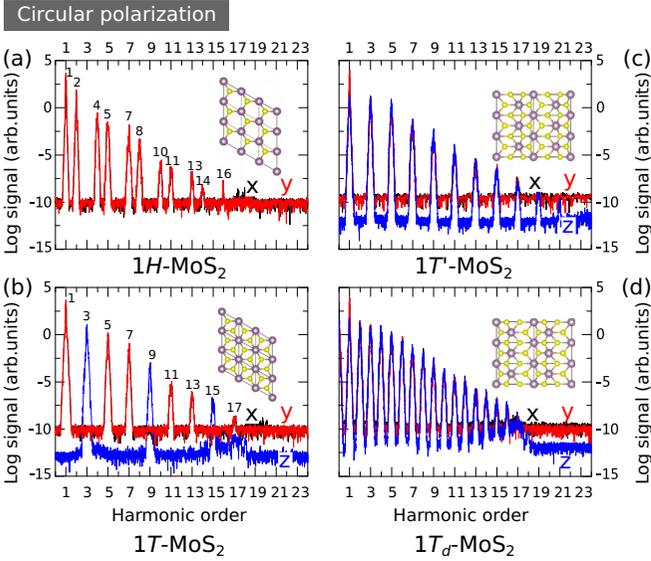
FIG. 2. High harmonic signals from MoS_2 when the laser field is circularly polarized. (a) The harmonic signals from $1H$ MoS_2, where the harmonic signals along the x and y axes appear while the harmonic signals along the z axis disappear. Interestingly, the harmonic order is $3n \pm 1$. (b) The harmonic signals from $1T$ MoS_2. In contrast to panel (a), the even harmonics disappear owing to the inversion symmetry and additional harmonics are induced along the z axis. (c) The harmonic signals from $1T'$ MoS_2. Only odd harmonics appear. (d) The harmonic signals from $1T_d$ MoS_2. Even and odd harmonics coexist. All the parameters of laser pulse are the same as those in Fig. 1.

V. PHYSICS BEHIND HIGH HARMONIC GENERATION IN MoS₂

The above findings are interesting, but the underlying mechanism has not been fully understood [6]. In $1H$ MoS_2, we see that the selective even harmonics only appear for a few particular polarization configurations. Moreover, the $3n$-order harmonics disappear for the in-plane polarization components when the laser field is circularly polarized. This means that some even harmonics are not protected by the Berry curvature under the σ light [3,25].

Our dynamic density matrix ρ deduced from the Liouville equation indeed includes the complete information of the system (i.e., the interband and intraband transitions). More importantly, it also takes into account the crystal symmetry through $\mathcal{H}_I(t) = \sum_i O_i \hat{\mathbf{P}} \cdot \mathbf{A}(t)$, where O_i is the symmetry operation of a crystal, $\hat{\mathbf{P}}$ is the momentum operator, and $\mathbf{A}(t)$ is the vector potential of laser field. Importantly, we find that the symmetry operations O_i should be further classified into subgroups (SGs), depending on the laser polarization. In this way, the nth order of the time-dependent macroscopic polarization can be simplified as

$$P^{(n)}(t) = \gamma \sum_{SG} \sum_{i \in SG} O_i \hat{\mathbf{P}} \cdot \mathbf{A}^{(n)}(t), \qquad (2)$$

where γ is the proportionality coefficient which has a complex expression [26,27]. Commonly, O_i and $\hat{\mathbf{P}}$ cannot commute.

Thus, the symmetry operation O_i can act not only on the momentum operator $\hat{\mathbf{P}}$ but also on the laser vector field $\mathbf{A}(t)$.

In the following, we examine $1H$ MoS_2 under σ light excitation. The cases for the other three phases are presented in the Supplemental Material [22]. When the laser field is circularly polarized, the 12 symmetry operations of $1H$ MoS_2 should be classified into two subgroups SG_I and SG_{II}, as listed in Table SII of the Supplemental Material [22]. Here, we take SG_I as an example. SG_I has six symmetry operations: $E, C_3^1, C_3^2, \sigma_{xy}, \widetilde{C}_3^1,$ and $\widetilde{C}_3^2$. For in-plane σ light, no symmetry operation within SG_I changes the polarization direction of the harmonics, and thus only one unit is formed [22,28]. To ease the complexity of the calculation, we choose a single k point close to the Γ point to demonstrate the effect of the symmetry operations on HHG signals. Figure 3 shows the symmetry-operation-resolved harmonic signals. If we only employ the identity operation E, we see that both even and odd harmonics appear both in-plane [Fig. 3(a)] and out-of-plane [Fig. 3(f)]. This situation is the same when only the symmetry operations C_3^1 and C_3^2 are present [see black lines in Figs. 3(b) and 3(g)].

However, when we sum over the signals generated under $E, C_3^1,$ and C_3^2, only in-plane harmonics whose orders are $3n + 1$ and $3n + 2$ survive [Fig. 3(c)]. This means that the symmetry adapted polarization cancels out the harmonics of other frequencies. Within the same SG_I, symmetry operations $\sigma_{xy}, \widetilde{C}_3^1,$ and $\widetilde{C}_3^2$ have the same effect [Fig. 3(d)]. Thus, when we sum over all symmetry-adapted polarizations, we only have $3n + 1$ and $3n + 2$ orders of harmonics [Fig. 3(e)]. However, this exact summation cancels out the out-of-plane signal along the z axis [see Fig. 3(j)]. It is also noticed that similar selection rules have been reported in molecules [29]. But the understanding of the underlying physics has not been given under the classification of the group symmetry.

We can understand the above finding analytically [30,31]. The circularly polarized laser pulse has a vector potential as $\mathbf{A}(t) = A_0 \exp(-t^2/\tau^2) \cos(\varphi \pm \omega t)\hat{\mathbf{e}}_{xy}$, where A_0 is the amplitude, τ is the pulse duration, and $\varphi = \pi/4$ is the phase factor. For harmonic generation, the Gaussian pulse shape only changes the profile of the harmonic signal but does not shift its frequency. For simplicity, we drop this term in the following analysis. Compared with the linearly polarized light, the phase factor φ provides an additional degree of freedom to modulate the selection rules of HHG [22]. This dramatically changes the harmonic orders, which enables us to distinguish the crystalline phases of MoS_2. The nth-order electric polarization is proportional to the nth power of the vector potential $\mathbf{A}(t)$. Following the same ideas in Eq. (2), we expand the polarization as

$$P_C^{(n)}(t) = \eta \sum_{SG} \sum_{i \in SG} O_i \hat{P} \frac{1}{2^n} \sum_{k=0}^{n} C_n^k \cos[(2k - n)(\varphi \pm \omega t)],$$

$$(3)$$

where η is the reduced parameter. The in-plane polarization component of the harmonics can be further clarified by introducing an operation such as [30]

$$O_{xy}^C = (\varphi_i \rightarrow +2\pi/3,\ t \rightarrow +T/3). \qquad (4)$$
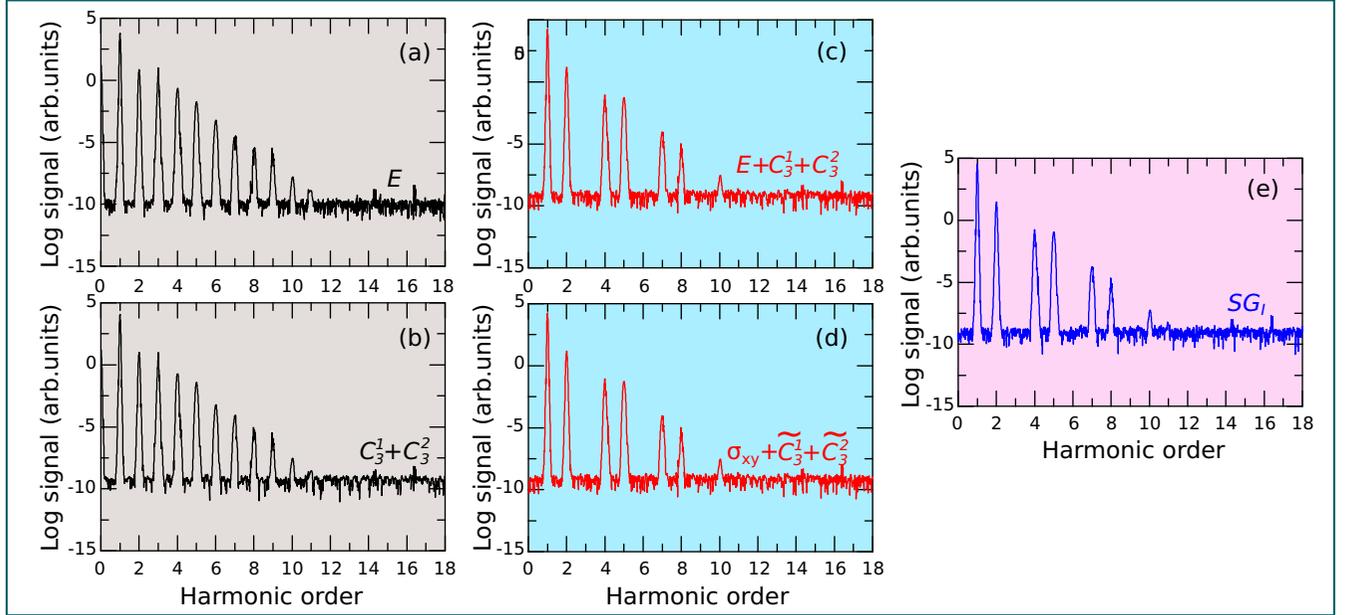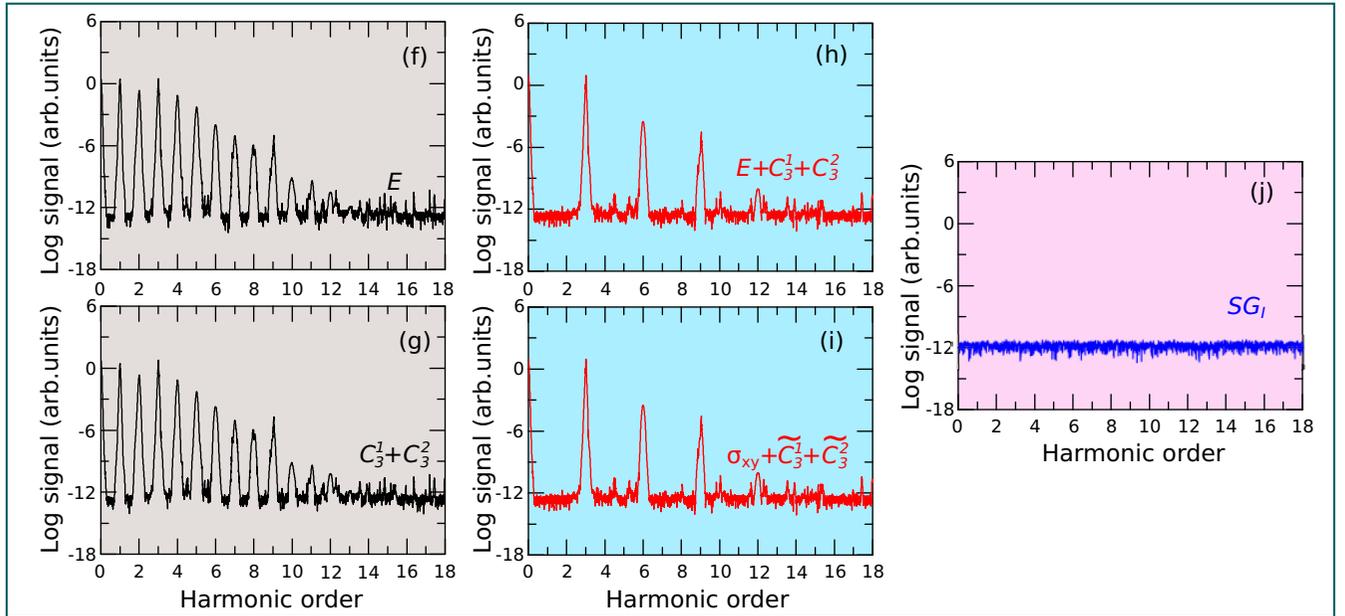
FIG. 3. Manifestation of group symmetry in HHG from $1H$ MoS$_2$ at the Γ point in the momentum space. Under the in-plane (xy) σ-polarized light, the symmetry-adapted HHG signals along the (a)–(e) x and (f)–(j) z axes have a distinctive dependence on symmetry operations. Data in panel (e) are the sum of those of panels (c) and (d) before Fourier transform. Data in panel (j) are the sum of those of panels (h) and (i), where the out-of-plane mirror reflection cancels out the harmonic signals. The parameters of the laser pulse are the same as in Fig. 1.

This operation of Eq. (4) requires the phase factor φ_i to be changed, which is absent for the linearly polarized laser field [22]. The change of one third of a period both in the phase factor φ_i and in the time t originates from the in-plane threefold rotational symmetry C_3^n. If the crystal has another in-plane rotational symmetry, the order properties of HHG will be changed accordingly [31].

Based on the operation in Eq. (4), the harmonic signals constrained from Eq. (3) appear if and only if

$$\cos\left[(2k-n)(\varphi \pm \omega t)\right] = \cos\left\{(2k-n)(\varphi \pm \omega t\right.$$
$$\left. + \left[1 \pm (2k-n)\right]2\pi/3\right\}. \quad (5)$$

Equation (4) dominates the selection rules of HHG under the circularly polarized laser, giving rise to the $(3n \pm 1)$-order harmonics constrained by Eq. (5). Compared with the linearly polarized laser, the circularly polarized laser requires the selective vanishing of odd or even harmonics. This largely extends the application of HHG. All the above discoveries also hold for the other three phases: $1T$, $1T'$, and $1T_d$ [22].

VI. ROLE OF BERRY CURVATURE

Liu and coauthors reported that the Berry curvature dominates the even harmonics [3], where only the intraband nonlinear current is taken into account. In contrast, in our calculations, we find that both the interband and intraband transitions contribute to the even harmonics due to breaking of the inversion symmetry. Therefore, it seems necessary to reevaluate the influence of the Berry curvature on the even HHG.

Among the four crystalline phases of MoS_2, the nonzero Berry curvature only appears in the $1H$ or $1T_d$ structure [32]. Here, we take $1H$ MoS_2 to demonstrate the role of Berry curvature on HHG. According to semiclassical theory, the effect of the Berry curvature on HHG under the circularly polarized laser field can be evaluated by [32–34]

$$v(t) = \frac{\omega_B}{a} \sum_{n=1}^{\infty} \sum_{m=1}^{\infty} \Omega_n (-1)^m J_{2m-1}\left(\frac{n\omega_B}{\omega}\right) \{\sin\left[2m(\varphi \pm \omega t)\right] - \sin\left[(2m-2)(\varphi \pm \omega t)\right]\}, \tag{6}$$

where Ω_n is the Fourier coefficient from expanding the Berry curvature, J_l is the Bessel function of the first kind of order l, a is the lattice constant of the crystal along the direction of the applied laser field, and $\omega_B = eE_0 a/\hbar$ is the Bloch frequency. The inversion symmetry breaking enters the Berry curvature as it is expanded in the sine Fourier series. According to the above analysis of the effect of crystal symmetry on the interband and intraband transitions, Eq. (6) should be invariant under the operation of the type: $\varphi_i \to +2\pi/3$, $t \to +T/3$. As a result, the Berry curvature gives rise to the $(6n \pm 2)$-order harmonics when the laser field is circularly polarized, being covered in the above-calculated HHG. This result is very important and reveals that some even harmonics (i.e., order $6n$) would disappear under the circularly polarized laser field. In other words, the even harmonics are not necessarily protected by the Berry curvature. However, the intrinsic selec-

tion rule still works, which is rooted in the crystal symmetry [6]. In magnetically doped topological insulators, we also find that the broken inversion symmetry induces even harmonics, which stems from the effect of spin-orbit coupling [35]. In the meantime, we cannot exclude the appearance of even harmonics from the interband polarization because the electron transition immediately responds to the irradiation of the laser pulse and then the intraband electronic dynamics occurs. In fact, the appearance of even harmonics from the Berry curvature is dominated by the breaking of inversion symmetry regardless of the interband or intraband contribution.

VII. CONCLUSION

We have demonstrated that HHG from monolayer MoS_2 contains rich structural information about its crystalline symmetries and electronic properties. To understand the underlying physics, we classify the symmetry operations into several subgroups that preserve the laser polarization. The symmetry classification is different for the circularly and linearly polarized lasers. For example, in $1H$ MoS_2, we classify the 12 symmetry operations into three subgroups for linearly polarized light. Each subgroup contains four symmetry operations (see Supplemental Material for more details [22]). However, we can only classify the 12 symmetry operations into two subgroups for the circularly polarized light and each subgroup has six symmetry operations. This leads to different HHG for the circularly and linearly polarized lasers. Our results suggest that the electronic property, the Berry curvature, the interband transitions, and the intraband transitions cannot alter the intrinsic selection rules of HHG, which are instead dictated by the crystal symmetry. These findings demonstrate a feasible way to characterize the crystalline phases of MoS_2 through the emitted HHG.

[1] S. Ghimire and D. A. Reis, High-harmonic generation from solids, Nat. Phys. **15**, 10 (2019).

[2] Y. Yang, K. Lu, A. Manjavacas, T. S. Luk, H. Liu, K. Kelley, J.-P. Maria, E. L. Runnerstrom, M. B. Sinclair, S. Ghimire, and I. Brener, High-harmonic generation from an epsilon-near-zero material, Nat. Phys. **15**, 1022 (2019).

[3] H. Liu, Y. Li, Y. S. You, S. Ghimire, T. F. Heinz, and D. A. Reis, High-harmonic generation from an atomically thin semiconductor, Nat. Phys. **13**, 262 (2017).

[4] F. Krausz and M. Ivanov, Attosecond physics, Rev. Mod. Phys. **81**, 163 (2009).

[5] P. B. Corkum and F. Krausz, Attosecond science, Nat. Phys. **3**, 381 (2007).

[6] O. Neufeld, D. Podolsky, and O. Cohen, Floquet group theory and its application to selection rules in harmonic generation, Nat. Commun. **10**, 405 (2019).

[7] J. Shi, Y.-Q. Bie, W. Chen, S. Fang, J. Han, Z. Cao, T. Taniguchi, K. Watanabe, V. Bulovic, E. Kaxiras, P. Jarillo-Herrero, and K. A. Nelson, Terahertz-driven irreversible topological phase transition in two-dimensional MoTe₂, arXiv:1910.13609.

[8] E. J. Sie, C. M. Nyby, C. D. Pemmaraju, S. J. Park, X. Shen, J. Yang, M. C. Hoffmann, B. K. Ofori-Okai, R. Li, A. H. Reid,

S. Weathersby *et al.*, An ultrafast symmetry switch in a Weyl semimetal, Nature (London) **565**, 61 (2019).

[9] I. Al-Naib, J. E. Sipe, and M. M. Dignam, High harmonic generation in undoped graphene: Interplay of inter- and intraband dynamics, Phys. Rev. B **90**, 245423 (2014).

[10] S.-Y. Hong, J. I. Dadap, N. Petrone, P.-C. Yeh, J. Hone, and R. M. Osgood, Jr., Optical Third-Harmonic Generation in Graphene, Phys. Rev. X **3**, 021014 (2013).

[11] N. Yoshikawa, T. Tamaya, and K. Tanaka, High-harmonic generation in graphene enhanced by elliptically polarized light excitation, Science **356**, 736 (2017).

[12] M.-X. Guan, C. Lian, S.-Q. Hu, H. Liu, S.-J. Zhang, J. Zhang, and S. Meng, Cooperative evolution of intraband and interband excitations for high-harmonic generation in strained MoS_2, Phys. Rev. B **99**, 184306 (2019).

[13] T. Tamaya, S. Konabe, and S. Kawabata, Orientation dependence of high-harmonic generation in monolayer transition metal dichalcogenides, arXiv:1706.00548v1.

[14] N. Kumar, S. Najmaei, Q. Cui, F. Ceballos, P. M. Ajayan, J. Lou, and H. Zhao, Second harmonic microscopy of monolayer MoS_2, Phys. Rev. B **87**, 161403 (2013).

[15] L. M. Malard, T. V. Alencar, A. P. M. Barboza, K. F. Mak, and A. M. de Paula, Observation of intense second harmonic generation from MoS_2 atomic crystals, Phys. Rev. B **87**, 201401 (2013).

[16] Z. Sun, Y. Yi, T. Song, G. Clark, B. Huang, Y. Shan, S. Wu, D. Huang, C. Gao, Z. Chen *et al.*, Giant nonreciprocal second-harmonic generation from antiferromagnetic bilayer CrI_3, Nature (London) **572**, 497 (2019).

[17] K. F. Mak, C. Lee, J. Hone, J. Shan, and T. F. Heinz, Atomically Thin MoS_2: A New Direct-Gap Semiconductor, Phys. Rev. Lett. **105**, 136805 (2010).

[18] J. S. Sandoval, D. Yang, R. F. Frindt, and J. C. Irwin, Raman study and lattice dynamics of single molecular layers of MoS_2, Phys. Rev. B **44**, 3955 (1991).

[19] G. Eda, T. Fujita, H. Yamaguchi, D. Voiry, M. Chen, and M. Chhowalla, Coherent atomic and electronic heterostructures of single-layer MoS_2, ACS Nano **6**, 7311 (2012).

[20] X. Qian, J. Liu, L. Fu, and J. Li, Quantum spin Hall effect in two-dimensional transition metal dichalcogenides, Science **346**, 1344 (2014).

[21] G. P. Zhang, Y. H. Bai, and T. F. George, Energy- and crystal momentum-resolved study of laser-induced femtosecond magnetism, Phys. Rev. B **80**, 214415 (2009).

[22] For more detailed discussions and results of $1T$, $1T'$, and $1T_d$ MoS_2, please see Supplemental Material at http://link.aps.org/supplemental/10.1103/PhysRevB.101.144304 which also includes Refs. [36–41].

[23] G. P. Zhang, M. S. Si, M. Murakami, Y. H. Bai, and T. F. George, Generating high-order optical and spin harmonics from ferromagnetic monolayers, Nat. Commun. **9**, 3031 (2018).

[24] H. J. Simon and N. Bloembergen, Second-harmonic light generation in crystals with natural optical activity, Phys. Rev. **171**, 1104 (1968).

[25] S.-Y. Xu, Q. Ma, H. Shen, V. Fatemi, S. Wu, T.-R. Chang, G. Chang, A. M. M. Valdivia, C.-K. Chan, Q. D. Gibson *et al.*,

Electrically switchable Berry curvature dipole in the monolayer topological insulator WTe_2, Nat. Phys. **14**, 900 (2018).

[26] C. L. Tang and H. Rabin, Selection rules for circularly polarized waves in nonlinear optics, Phys. Rev. B **3**, 4025 (1971).

[27] Y. Tokura and N. Nagaosa, Nonreciprocal responses from non-centrosymmetric quantum materials, Nat. Commun. **9**, 3740 (2018).

[28] G. P. Zhang and Y. H. Bai, Magic high-order harmonics from a quasi-one-dimensional hexagonal solid, Phys. Rev. B **99**, 094313 (2019).

[29] R. Baer, D. Neuhauser, P. R. Zdanska, and N. Moiseyev, Ionization and high-order harmonic generation in aligned benzene by a short intense circularly polarized laser pulse, Phys. Rev. A **68**, 043406 (2003).

[30] O. E. Alon, V. Averbukh, and N. Moiseyev, Selection Rules for the High Harmonic Generation Spectra, Phys. Rev. Lett. **80**, 3743 (1998).

[31] N. Saito, P. Xia, F. Lu, T. Kanai, J. Itatani, and N. Ishii, Observation of selection rules for circularly polarized fields in high-harmonic generation from crystalline solid, Optica **4**, 1333 (2017).

[32] D. Xiao, M. C. Chang, and Q. Niu, Berry phase effects on electronic properties, Rev. Mod. Phys. **82**, 1959 (2010).

[33] A. Chernikov, T. C. Berkelbach, H. M. Hill, A. Rigosi, Y. Li, O. B. Aslan, D. R. Reichman, M. S. Hybertsen, and T. F. Heinz, Exciton Binding Energy and Nonhydrogenic Rydberg Series in Monolayer WS_2, Phys. Rev. Lett. **113**, 076802 (2014).

[34] T. T. Luu and H. J. Wörner, Measurement of the Berry curvature of solids using high-harmonic spectroscopy, Nat. Commun. **9**, 916 (2018).

[35] Lei Jia, Zhiya Zhang, D. Z. Yang, M. S. Si, G. P. Zhang, and Y. S. Liu, High harmonic generation in magnetically-doped topological insulators, Phys. Rev. B **100**, 125144 (2019).

[36] P. Blaha, K. Schwarz, G. K. H. Madsen, D. Kvasnicka, and J. Luitz, *WIEN2k, An Augmented Plane Wave + Local Orbitals Program for Calculating Crystal Properties* (Karlheinz Schwarz, Techn. Universität Wien, 2001).

[37] D. Xiao, G.-B. Liu, W. Feng, X. Xu, and W. Yao, Coupled Spin and Valley Physics in Monolayers of MoS_2 and Other Group-VI Dichalcogenides, Phys. Rev. Lett. **108**, 196802 (2012).

[38] P. Blaha, K. Schwarz, P. Sorantin, and S. B. Trickey, Full-potential, linearized augmented plane wave programs for crystalline systems, Comput. Phys. Commun. **59**, 399 (1990).

[39] J.-S. You, S. Fang, S.-Y. Xu, E. Kaxiras, and T. Low, Berry curvature dipole current in the transition metal dichalcogenides family, Phys. Rev. B **98**, 121109(R) (2018).

[40] R. Kappera, D. Voiry, S. E. Yalcin, W. Jen, M. Acerce, S. Torrel, B. Branch, S. Lei, W. Chen, S. Najmaei, J. Luo, P. M. Ajayan, G. Gupta, A. D. Mohite, and M. Chhowalla, Metallic $1T$ phase source/drain electrodes for field effect transistors from chemical vapor deposited MoS_2, APL Mater. **2**, 092516 (2014).

[41] J. P. Perdew, K. Burke, and M. Ernzerhof, Generalized Gradient Approximation Made Simple, Phys. Rev. Lett. **77**, 3865 (1996).